# Photoneutron Cross Sections for Unstable Neutron-Rich Oxygen Isotopes

A. Leistenschneider,[1] T. Aumann,[2] K. Boretzky,[3] D. Cortina,[2] J. Cub,[4] U. Datta Pramanik,[2] W. Dostal,[3] Th. W. Elze,[1] H. Emling,[2] H. Geissel,[2] A. Grünschloß,[1] M. Hellstr,[2] R. Holzmann,[2] S. Ilievski,[2] N. Iwasa,[2] M. Kaspar,[2] A. Kleinböhl,[1] J. V. Kratz,[3] R. Kulessa,[5] Y. Leifels,[2] E. Lubkiewicz,[5] G. Münzenberg,[2] P. Reiter,[6] M. Rejmund,[2] C. Scheidenberger,[2] C. Schlegel,[4] H. Simon,[4] J. Stroth,[1] K. Sümmerer,[2] E. Wajda,[5] W. Walús,[5] and S. Wan[2]

[1]*Institut für Kernphysik, Johann Wolfgang Goethe-Universität, D-60486 Frankfurt, Germany*
[2]*Gesellschaft für Schwerionenforschung (GSI), D-64291 Darmstadt, Germany*
[3]*Institut für Kernchemie, Johannes Gutenberg-Universität, D-55099 Mainz, Germany*
[4]*Institut für Kernphysik, Technische Universität, D-64289 Darmstadt, Germany*
[5]*Instytut Fizyki, Uniwersytet Jagelloński, PL-30-059 Kraków, Poland*
[6]*Sektion Physik, Ludwig-Maximilians-Universität, D-85748 Garching, Germany*

(Received 19 December 2000)

The dipole response of stable and unstable neutron-rich oxygen nuclei of masses $A = 17$ to $A = 22$ has been investigated experimentally utilizing electromagnetic excitation in heavy-ion collisions at beam energies about 600 MeV/nucleon. A kinematically complete measurement of the neutron decay channel in inelastic scattering of the secondary beam projectiles from a Pb target was performed. Differential electromagnetic excitation cross sections $d\sigma/dE$ were derived up to 30 MeV excitation energy. In contrast to stable nuclei, the deduced dipole strength distribution appears to be strongly fragmented and systematically exhibits a considerable fraction of low-lying strength.

DOI: 10.1103/PhysRevLett.86.5442 PACS numbers: 21.10.Re, 24.30.–v, 25.60.–t, 27.20.+n

The study of the response of a nucleus to an external nuclear or electromagnetic field is one key to understanding the properties of the nuclear many-body system. At excitation energies above the particle threshold, the nuclear response of stable nuclei is dominated by collective vibrations of various multipolarities, the giant resonances. How the giant resonance strength evolves when going from stable to exotic weakly bound nuclei with extreme neutron-to-proton ratios is presently under much discussion [1–6]. For neutron-rich nuclei, model calculations predict pronounced effects, in particular a redistribution of the strength towards lower excitation energies well below the giant resonance region. The predicted strength functions depend strongly on the effective forces used in the calculations. In turn, measurements of the multipole continuum response of exotic nuclei can yield important information on the isospin dependent part of the in-medium nucleon-nucleon interaction [7].

Systematic experimental information on the multipole response of exotic nuclei, however, is still not available. For some light halo nuclei, low-lying dipole strength was observed in electromagnetic dissociation measurements [8–11]. For the one-neutron halo nuclei $^{11}$Be [9,12] and $^{19}$C [11], the observed dipole strength at very low excitation energies was interpreted as a quantum-mechanical threshold effect, involving nonresonant transitions of the valence neutron into the continuum [3,13]. For the nuclei $^{6}$He and $^{11}$Li, a coherent dipole vibration of the two halo neutrons against the core was discussed as well [14–18]. The appearance of a collective soft-dipole resonance in general was predicted for heavier neutron-rich systems [19,20], located at excitation energies below the giant dipole resonance (GDR) [19]. Such a mode, in literature sometimes referred to as pygmy resonance, may arise if less tightly bound valence neutrons vibrate against the residual core. We note in passing that a systematic appearance of low-lying dipole strength in neutron-rich nuclei may concern astrophysical aspects, e.g., calculations of element abundancies in the $r$-process of the nucleosynthesis as shown in [21].

In a first attempt to study giant resonances and lower lying modes in exotic nuclei, we investigated systematically the dipole strength distributions of all neutron-rich oxygen isotopes up to $^{22}$O. $^{16}$O is a strongly bound doubly magic nucleus. For the heavier isotopes, one may expect a decoupling of the valence neutrons from the inert $^{16}$O core. The separation energy of the last neutron is 7–8 MeV for the even isotopes $A = 18$–$22$, and about 4 MeV for the odd isotopes, to be compared to 16 MeV for $^{16}$O. Thus the neutron-rich oxygen isotopes might be good candidates for a collective soft-dipole excitation.

As the experimental tool, we use the electromagnetic excitation of fast projectiles by high $Z$ targets. Similar to photoabsorption, this process is mostly sensitive to electric dipole transitions with only small E2 contributions. For example, 10% of the energy-weighted sum rule for E1 and E2 transitions placed arbitrarily at an excitation energy of 12 MeV leads to electromagnetic excitation cross sections of 66 and 3.7 mb, respectively (calculated for 600 MeV/nucleon $^{18}$O on a Pb target). It was demonstrated for stable nuclei [22] that the dipole strength function can be deduced quantitatively from a measurement of the differential electromagnetic dissociation cross section essentially without free parameters by applying semiclassical calculations [23,24]. The high secondary beam energy of about 600 MeV/nucleon allows for the

 0031-9007/01/86(24)/5442(4)$15.00 

first time the investigation of dipole transitions in exotic nuclei up to 30 MeV in excitation energy.

The radioactive beams were produced in a fragmentation reaction of a primary $^{40}$Ar beam delivered by the synchrotron SIS at GSI, Darmstadt, impinging on a beryllium target. Secondary oxygen projectiles were separated using the fragment separator [25] and identified uniquely by means of energy-loss and time-of-flight measurements. Behind the Pb (1.82 g/cm$^2$) target, the fragments were deflected by a large-gap dipole magnet. By using energy-loss and time-of-flight measurements, as well as position measurements in front of and behind the dipole magnet, the nuclear charge, velocity, scattering angle, and mass of the fragments can be determined. Neutrons emitted from the excited projectile or excited projectilelike fragments are kinematically focused into the forward direction and detected with high efficiency ($\approx$90%) in the LAND neutron detector [26], placed at 0° about 11 m downstream from the target and covering horizontal and vertical angular ranges of about $\pm$80 mrad. To detect the $\gamma$ rays, the target was surrounded by the $4\pi$ Crystal Ball spectrometer, consisting of 160 NaI detectors. The excitation energy prior to decay is obtained by reconstructing the invariant mass. To disentangle electromagnetic excitation from nuclear interaction processes, we measured the fragment mass with good resolution ($\sigma_A \approx 0.1$) and compared it to the number of neutrons emitted in the forward direction: In the case of electromagnetic excitation, the difference in mass number between the projectile and fragment equals the number of neutrons. In contrast, nucleons which are knocked out in nuclear reactions are scattered to large angles and are not detected in LAND. The remaining nuclear background was determined from a measurement with a C target and scaled by a factor of 2.1. This scaling factor between nuclear cross sections from the C and Pb targets was determined from the measured cross section ratios for fragmentation products originating from purely nuclear processes. Details of the experimental procedures will be published in a forthcoming article.

In Fig. 1, the extracted differential cross section for the electromagnetic excitation into the continuum followed by neutron decay is shown for $^{18}$O. For the stable nucleus $^{18}$O, photoabsorption data exist [27–29] which we compare with our electromagnetic dissociation results obtained under identical conditions as the radioactive isotopes $^{20}$O and $^{22}$O. The electromagnetic excitation cross section calculated from the measured photoneutron cross sections of Ref. [27] is shown in Fig. 1 by the dashed curve, where effects due to our instrumental response were taken into account. The comparison with the present data (open symbols) shows very good agreement above 11 MeV excitation energy, while, below 11 MeV, we observe a larger cross section. A better overall agreement is observed in the comparison with the cross sections obtained from the data of Ref. [28] if their photoneutron data are scaled by a factor 0.8 (solid curve after, grey curve before, convolution with the instrumental response). The excitation energy

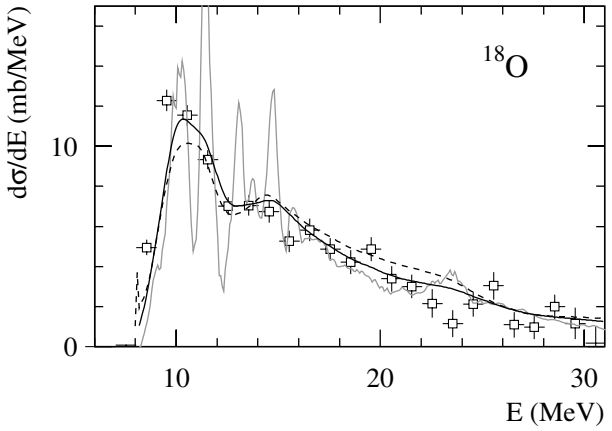


FIG. 1. Differential cross sections for electromagnetic excitation followed by neutron decay as a function of excitation energy $E$ for $^{18}$O projectiles impinging on a Pb target. The data are compared with cross sections calculated from the measured photoneutron cross sections from Refs. [27,28]. The solid curves show the cross sections resulting from the data of Ref. [28] (scaled by a factor of 0.8) before (grey line) and after (black line) convolution with our experimental response. The dashed curve is obtained from the data of Ref. [27].

resolution $\sigma_E$ in our measurements can be well approximated by $\sigma_E = 0.20 + 0.11(E - S)$ [MeV]; $S$ denotes the one neutron separation energy. Thus, the individual resonances seen in photoabsorption are hardly resolved.

From the electromagnetic dissociation cross sections, we extract the photoneutron cross sections $\sigma_{(\gamma,xn)}$ by applying semiclassical calculations [23,24]. Figure 2 shows the deduced $\sigma_{(\gamma,xn)}$ for $^{20,22}$O, where neutron multiplicities up to $x = 3$ are included. For comparison, the photoneutron cross sections are also shown for the stable nucleus $^{16}$O (upper frame) as measured with real photons [30]. Evidently, the dipole response changes significantly due to the presence of the valence neutrons. Most noticeable is the sizable dipole absorption cross section below the GDR energy region. The data are compared to a large-scale shell model calculation by Sagawa and Suzuki [4] using the Warburton-Brown interaction WB10 (see Fig. 2). The calculated photoabsorption cross sections were convoluted with the experimental resolution. Qualitatively, the shell model calculations reproduce the experimental observation of a redistribution of the E1 strength towards excitation energies below the GDR if compared to the doubly magic nucleus $^{16}$O. The experimental data for $^{20}$O and $^{22}$O exhibit sharp and somewhat broader resonances, respectively, both near the neutron separation threshold which, in the shell model calculations, appears somewhat shifted in excitation energy. Evidently, a set of systematic data as presented here provides a stringent test of the quality of extended microscopic calculations. From our measurement, we also obtained results for the odd isotopes $^{17,19,21}$O [31] for which theoretical calculations, however, are not available.

In the following, we compare the observed low-lying dipole strength to an absolute scale, a measure of which is provided by (model independent) sum rules. Such a

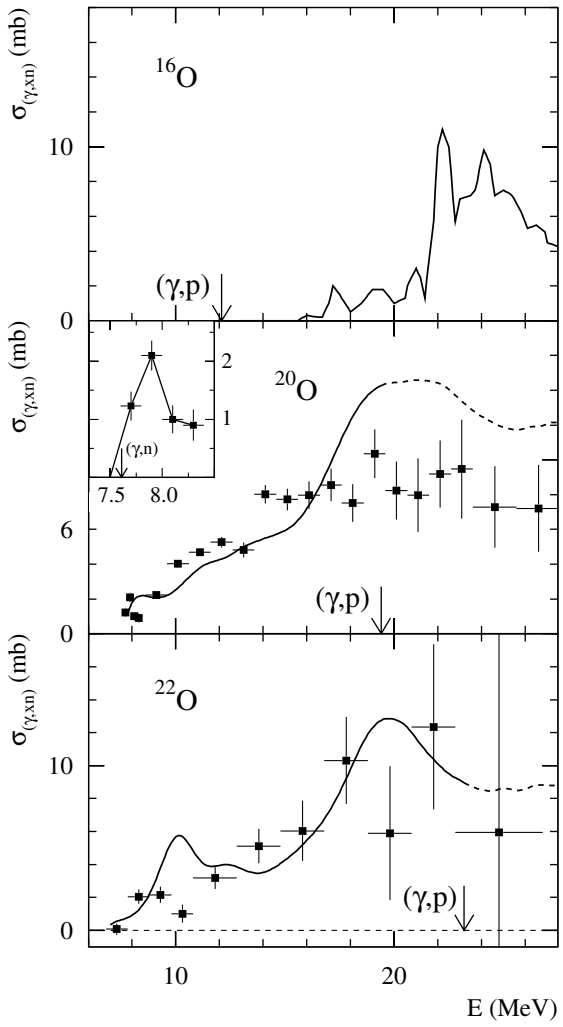


FIG. 2. Photoneutron cross sections $\sigma_{(\gamma,xn)}$ for $^{16}$O [30] (upper panel) and for the unstable isotopes $^{20,22}$O (lower panels) as extracted from the measured electromagnetic excitation cross section (symbols). The inset displays the cross section for $^{20}$O near the neutron threshold on an expanded energy scale. The thresholds for decay channels involving protons (which were not observed in the present experiment) are indicated by arrows. For $^{20,22}$O, the data are compared to the shell model calculations [4].

comparison may help to judge the degree of coherence of the dipole motion. Here, we consider the classical energy-weighted Thomas-Reiche-Kuhn sum rule $S_{\mathrm{TRK}} \sim NZ/A$ [32]. It may be decomposed into $S_{\mathrm{TRK}} = S_c + S_v + S_{\mathrm{rel}}$, i.e., into the strength of the dipole motion within the core ($S_c$), within the valence neutrons ($S_v$), and into the relative motion ($S_{\mathrm{rel}}$) between the core and the valence nucleons [33]. Naturally, we choose $^{16}$O as the core. In that case, $S_v$ vanishes and one obtains $S_{\mathrm{rel}} = S_{\mathrm{TRK}} Z_c/A_c \cdot N_v/N$. In the literature, this quantity is frequently referred to as the cluster sum rule, $S_{\mathrm{clus}} = S_{\mathrm{rel}}$ [33,34]; we adopt this notation in the following. We point out, however, that the assumption of a true cluster structure is not required for the application of this sum rule, as is evident from the above derivation. A meaningful application of the cluster sum rule requires only that the dipole strength distributions associated with the core and with the relative motion can be distinguished unambiguously, i.e., that the respective strength distributions are localized in distinct regions of excitation energy. Photoabsorption measurements in $^{16}$O [30] show that the giant dipole resonance is localized at excitation energies of 20–30 MeV. Since the neutron separation energies in the heavier oxygen isotopes are smaller than in $^{16}$O by a factor 2–4, one may expect the strength of the dipole motion of the valence particles relative to the core to be localized clearly below 20 MeV excitation energy, and we choose 15 MeV as an upper limit.

Figure 3 shows the energy-weighted dipole strength integrated over an excitation energy interval from the one-neutron separation energy up to 15 MeV plotted as a fraction of the classical and the cluster dipole sum rule. First, notice that this low-lying strength exhausts a sizable fraction of the classical sum rule, up to 12%. Second, it appears that the limit given by the cluster sum rule is nearly approached in the two lightest isotopes only, with a clear tendency of values decreasing with neutron number. Part of the missing strength may be localized at excitation energies below the neutron separation threshold, not covered in the present experiment. The shell model calculations, however, indicate that this portion of strength is rather small (less than 1% of the TRK sum rule). The missing strength most likely is localized at higher excitation energies, i.e., around the giant resonance domain. It means that a strict separation into core- and valence-neutron-dominated domains, underlying the above simplified picture, is not realized. This is also indicated if we plot the strength integrated up to 20 MeV, as shown in Fig. 3 as filled triangles. In this case, the cluster-sum-rule limit is exhausted for $^{21,22}$O, but for $^{18-20}$O the integrated strength clearly exceeds unity. Thus, core excitations already play a role in this energy region, while for $^{16}$O the integrated photoneutron cross section between 15 and 20 MeV corresponds only to 1.6% [30] of $S_{\mathrm{TRK}}$. To which extent the low-lying dipole strength observed in the neutron-rich oxygen isotopes involves coherent excitations or is due to single particle transitions must remain a subject of a detailed theoretical study. In this context, we refer to recent relativistic random-phase approximation calculations [35] for neutron-rich nuclei. Therein, in the case of oxygen isotopes, low-lying dipole strength is obtained comparable in magnitude to our experimental results, but it was concluded that low-energy transitions can essentially be assigned to single neutron particle-hole ($ph$) excitations rather than to coherent superpositions of many $ph$ configurations.

In summary, we have measured systematically for the first time the evolution of giant dipole strength with neutron excess for the neutron-rich oxygen isotopes from $A = 17$ to $A = 22$. Differential cross sections were derived up to an excitation energy of 30 MeV. For all neutron-rich oxygen isotopes investigated, the dipole strength appears to be strongly fragmented with a considerable fraction observed well below the giant dipole

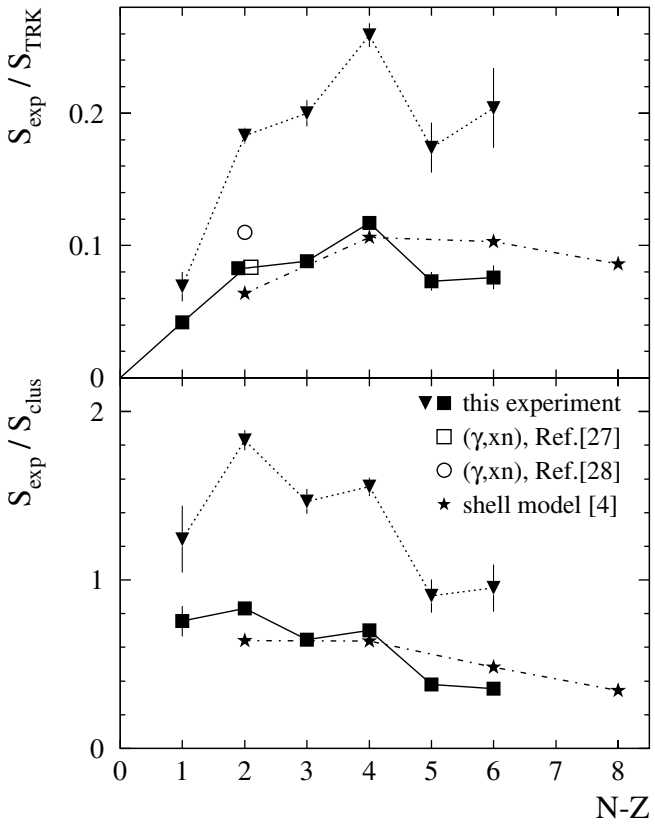


FIG. 3. Evolution of integrated (up to 15 MeV excitation energy) strength $S_{\text{exp}}$ in units of the TRK sum rule $S_{\text{TRK}}$ (upper panel) and of the cluster-sum-rule limit $S_{\text{clus}}$ (lower panel) for oxygen isotopes with the neutron excess $N - Z$. The data (filled squares) are compared to shell model calculations by Sagawa and Suzuki [4] (stars). The filled triangles display $S_{\text{exp}}$ if integrated up to 20 MeV excitation energy.

resonance, much in contrast to the dipole response of stable nuclei.

We thank H. Sagawa for providing the numerical data of the shell model calculations [4], and B. L. Berman for making the data of Ref. [28] available in tabular form. We also thank P. F. Bortignon and G. Colò for many discussions. This work was supported by the German Federal Minister for Education and Research (BMBF) under Contracts No. 06 OF 838 and No. 06 MZ 864, by GSI via Hochschulzusammenarbeitsvereinbarungen under Contracts OFELZK and MZKRAK, and partly supported by the Polish Committee of Scientific Research under Contract No. 2PB03 144 18.

[1] I. Hamamoto, H. Sagawa, and X. Z. Zhang, Phys. Rev. C **53**, 765 (1996); I. Hamamoto and H. Sagawa, Phys. Rev. C **53**, R1492 (1996).
[2] F. Ghielmetti, G. Colò, E. Vigezzi, P. F. Bortignon, and R. A. Broglia, Phys. Rev. C **54**, R2143 (1996).
[3] F. Catara, C. H. Dasso, and A. Vitturi, Nucl. Phys. **A602**, 181 (1996).
[4] H. Sagawa and T. Suzuki, Phys. Rev. C **59**, 3116 (1999).
[5] N. Dinh Dang, T. Suzuki, and A. Arima, Phys. Rev. C **61**, 064304 (2000).
[6] For a collection of recent theoretical articles we refer to the special issues on the following conference proceedings: *Giant Resonance Conference, Varenna 98,* edited by A. Bracco and P. F. Bortignon, Nucl. Phys. **A649** (1999); *Giant Resonance Conference, Osaka 2000,* Nucl. Phys. **A687** (2001).
[7] P. G. Reinhard, Nucl. Phys. **A649**, 305c (1999).
[8] T. Aumann *et al.,* Phys. Rev. C **59**, 1252 (1999).
[9] T. Nakamura *et al.,* Phys. Lett. B **331**, 296 (1994).
[10] D. Sackett *et al.,* Phys. Rev. C **48**, 118 (1993); F. Shimoura *et al.,* Phys. Lett. B **348**, 29 (1995); M. Zinser *et al.,* Nucl. Phys. **A619**, 151 (1997)..
[11] T. Nakamura *et al.,* Phys. Rev. Lett. **83**, 1112 (1999).
[12] R. Anne *et al.,* Nucl. Phys. **A575**, 125 (1994).
[13] P. G. Hansen and B. Jonson, Europhys. Lett. **4**, 409 (1987).
[14] K. Ikeda, Nucl. Phys. **A538**, 355c (1992).
[15] A. A. Korsheninnikov *et al.,* Phys. Rev. Lett. **78**, 2317 (1997).
[16] R. Kanungo, I. Tanihata, and C. Samanta, Prog. Theor. Phys. **102**, 1133 (1999).
[17] T. Suzuki, H. Sagawa, and P. F. Bortignon, Nucl. Phys. **A662**, 282 (2000).
[18] S. Nakayama *et al.,* Phys. Rev. Lett. **85**, 262 (2000).
[19] J. Chambers *et al.,* Phys. Rev. C **50**, R2671 (1994).
[20] Y. Suzuki, K. Ikeda, and H. Salto, Prog. Theor. Phys. **83**, 180 (1990).
[21] S. Goriely, Phys. Lett. B **436**, 10 (1998).
[22] T. Aumann, P. F. Bortignon, and H. Emling, Annu. Rev. Nucl. Part. Sci. **48**, 351 (1998); K. Boretzky *et al.,* Phys. Lett. B **384**, 30 (1996)..
[23] A. Winther and K. Alder, Nucl. Phys. **A319**, 518 (1979).
[24] C. A. Bertulani and G. Baur, Phys. Rep. **163**, 299 (1988).
[25] H. Geissel *et al.,* Nucl. Instrum. Methods. Phys. Res., Sect. B **70**, 286 (1992).
[26] T. Blaich *et al.,* Nucl. Instrum. Methods. Phys. Res., Sect. A **314**, 136 (1992).
[27] U. Kneissl *et al.,* Nucl. Phys. **A272**, 125 (1976).
[28] J. G. Woodworth *et al.,* Phys. Rev. C **19**, 1667 (1979).
[29] H. Harada *et al.,* Phys. Rev. Lett. **80**, 33 (1998).
[30] E. G. Fuller, Phys. Rep. **127**, 187 (1985); A. Vessière *et al.,* Nucl. Phys. **A227**, 513 (1974); B. L. Berman, At. Data Nucl. Data Tables **15**, 319 (1975).
[31] A. Leistenschneider *et al.* (to be published).
[32] A. Bohr and B. R. Mottelson, *Nuclear Structure* (Benjamin, London, 1975), Vol. 2.
[33] H. Sagawa and M. Honma, Phys. Lett. B **251**, 17 (1990).
[34] Y. Alhassid, M. Gai, and G. F. Bertsch, Phys. Rev. Lett. **49**, 1482 (1982).
[35] D. Vretenar *et al.,* Nucl. Phys. A (to be published).